

Supplementary Material of “Towards a More Balanced Reference Set Adaptation Method: First Results”

Luis A. Márquez-Vega

School of Engineering and Sciences
Tecnológico de Monterrey
Nuevo León, Mexico
a00832536@itesm.mx

Jesús Guillermo Falcón-Cardona

Department of Applied Mathematics and Systems
UAM-Cuajimalpa
Mexico City, Mexico
jfalcon@cua.uam.mx

Edgar Covantes Osuna

School of Engineering and Sciences
Tecnológico de Monterrey
Nuevo León, Mexico
edgar.covantes@tec.mx

I. QUALITATIVE RESULTS

Figures 1, 2, 3, and 4 show the approximation sets with the median IGD⁺ value among 30 independent runs obtained by IGD⁺-MaOEA-RS, A-IGD⁺-MaOEA-RS, R-IGD⁺-MaOEA-RS, and AR-IGD⁺-MaOEA-RS on DTLZ1-DTLZ7, DTLZ1⁻¹-DTLZ7⁻¹, IMOP1-IMOP3, and IMOP4-IMOP8, respectively. In Figure 1, it can be seen that AR-IGD⁺-MaOEA-RS is the only MOEA with a reference set adaptation method that preserves the good performance of IGD⁺-MaOEA-RS on MOPs with regular *Pareto fronts*. However, the maximum number of function evaluations used was insufficient to allow IGD⁺-MaOEA-RS to achieve its optimal distribution on DTLZ3 due to the multi-modality of the MOP. It also shows that the MOEAs with a reference set adaptation method, i.e., A-IGD⁺-MaOEA-RS, R-IGD⁺-MaOEA-RS, and AR-IGD⁺-MaOEA-RS improve the distribution of solutions obtained with IGD⁺-MaOEA-RS on DTLZ5-DTLZ7. Figure 2 shows that IGD⁺-MaOEA-RS generates approximation sets with many solutions crowded on some regions of the edge of *Pareto fronts* with inverted shapes. The use of reference set adaptation methods enhances the distribution of solutions of the IGD⁺-MaOEA-RS on these types of MOPs. However, it can be seen that the AR-IGD⁺-MaOEA-RS has difficulties covering some regions of the *Pareto fronts* with inverted convex shapes. Figure 3 and Figure 4 show the approximation sets on two- and three-objective MOPs from IMOP suite, respectively. It can be seen that the use of reference set adaptation methods improves the distribution of solutions obtained with IGD⁺-MaOEA-RS on MOPs with degenerated and disconnected *Pareto front* shapes. It can also be seen that all MOEAs cannot cover the *Pareto front* of the IMOP7.

Figures 5, 6, and 7 show the convergence graphs generated with the mean IGD⁺ value of 30 independent runs on MOPs from the DTLZ, DTLZ⁻¹, and IMOP suites, respectively. It can be seen that the reference set adaptation methods do not alter the convergence speed of IGD⁺-MaOEA-RS on most MOPs. However, Figure 7 shows that the approximation set obtained by AR-IGD⁺-MaOEA-RS converge more quickly

than other MOEAs on IMOP4. It can also be seen that the convergence speed of all MOEAs can be improved on some MOPs, especially on IMOP2, IMOP3, and IMOP4.

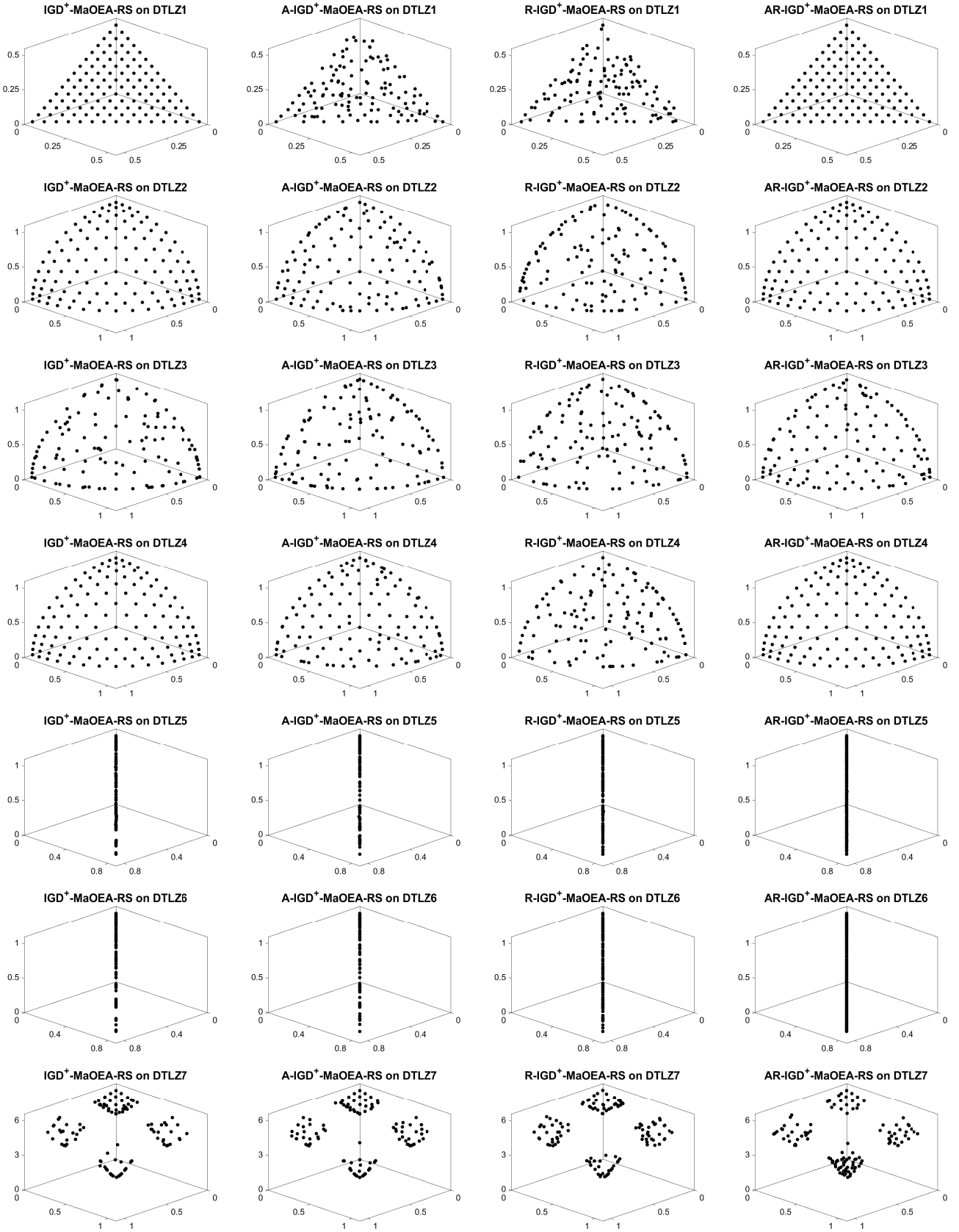


Fig. 1. Approximation sets with the median IGD⁺ value among 30 independent runs on DTLZ1-DTLZ7.

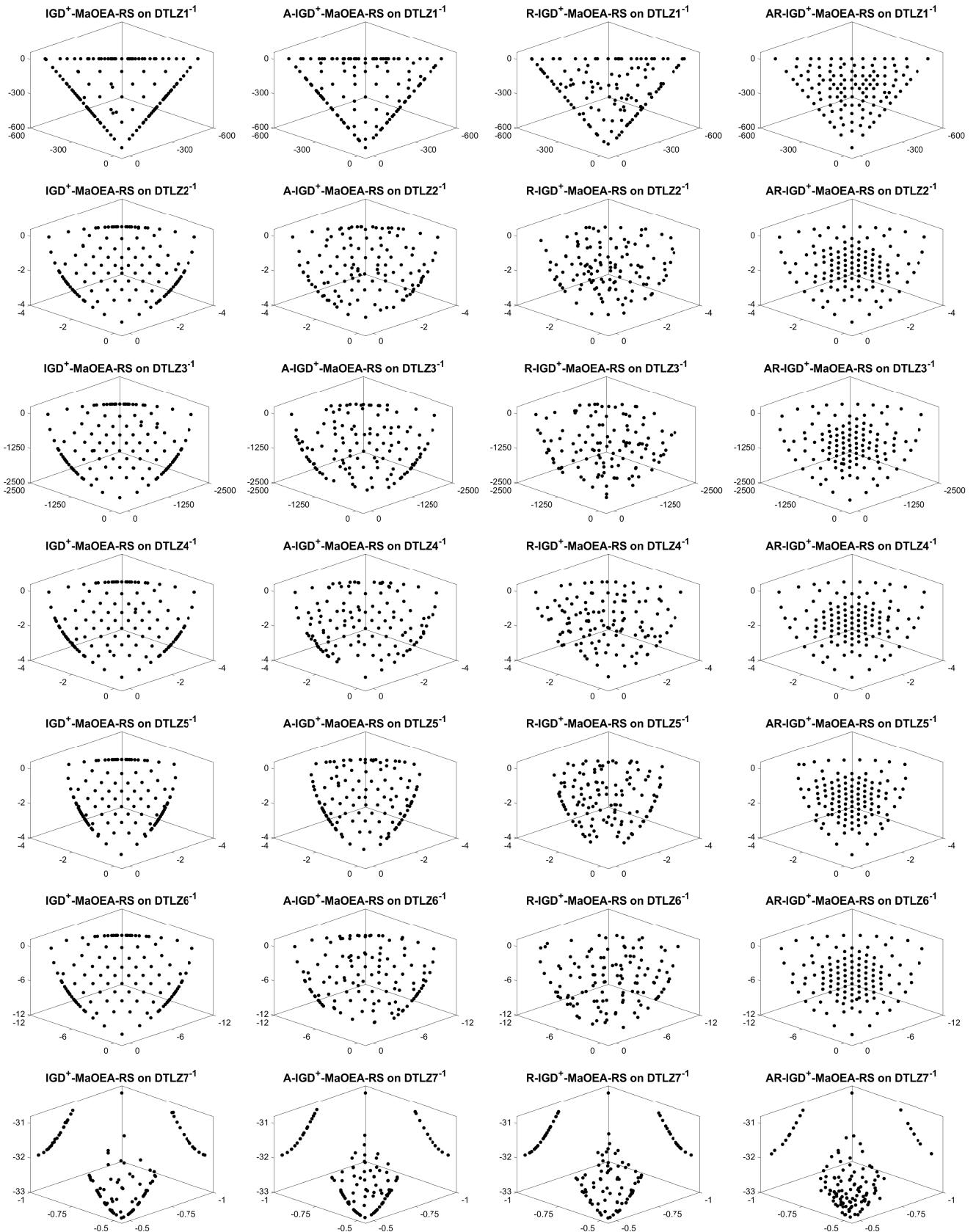


Fig. 2. Approximation sets with the median IGD⁺ value among 30 independent runs on DTLZ1⁻¹-DTLZ7⁻¹.

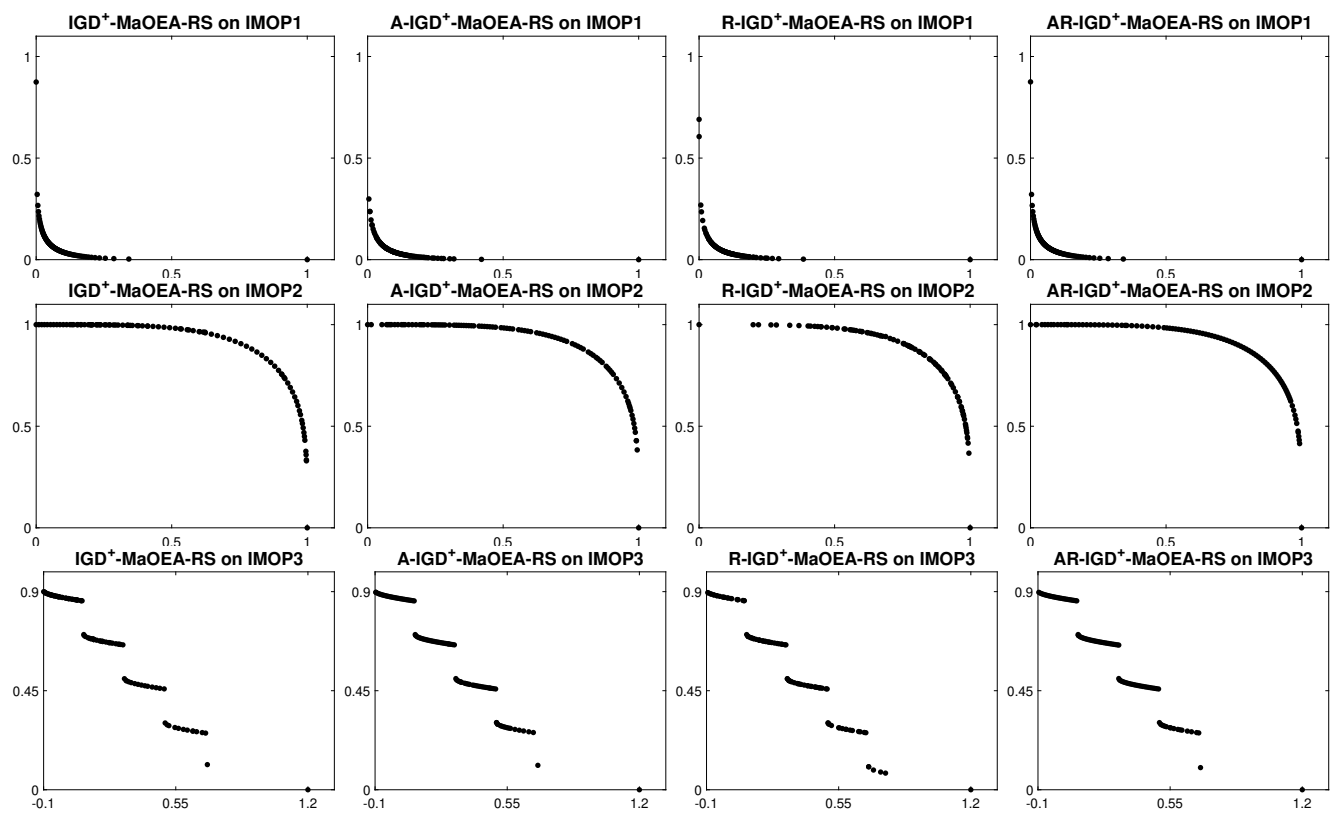


Fig. 3. Approximation sets with the median IGD^+ value among 30 independent runs on IMOP1-IMOP3.

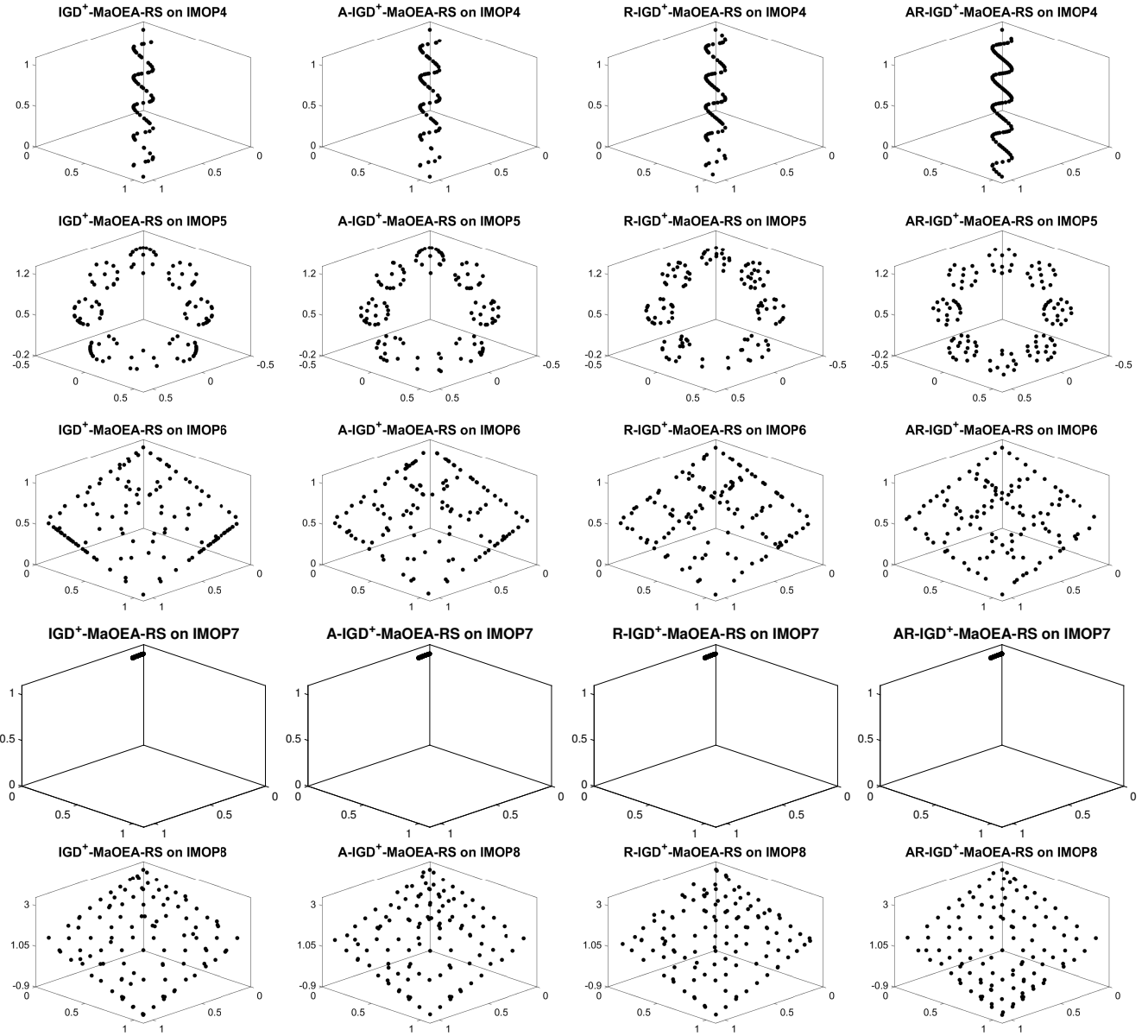


Fig. 4. Approximation sets with the median IGD⁺ value among 30 independent runs on IMOP4-IMOP8.

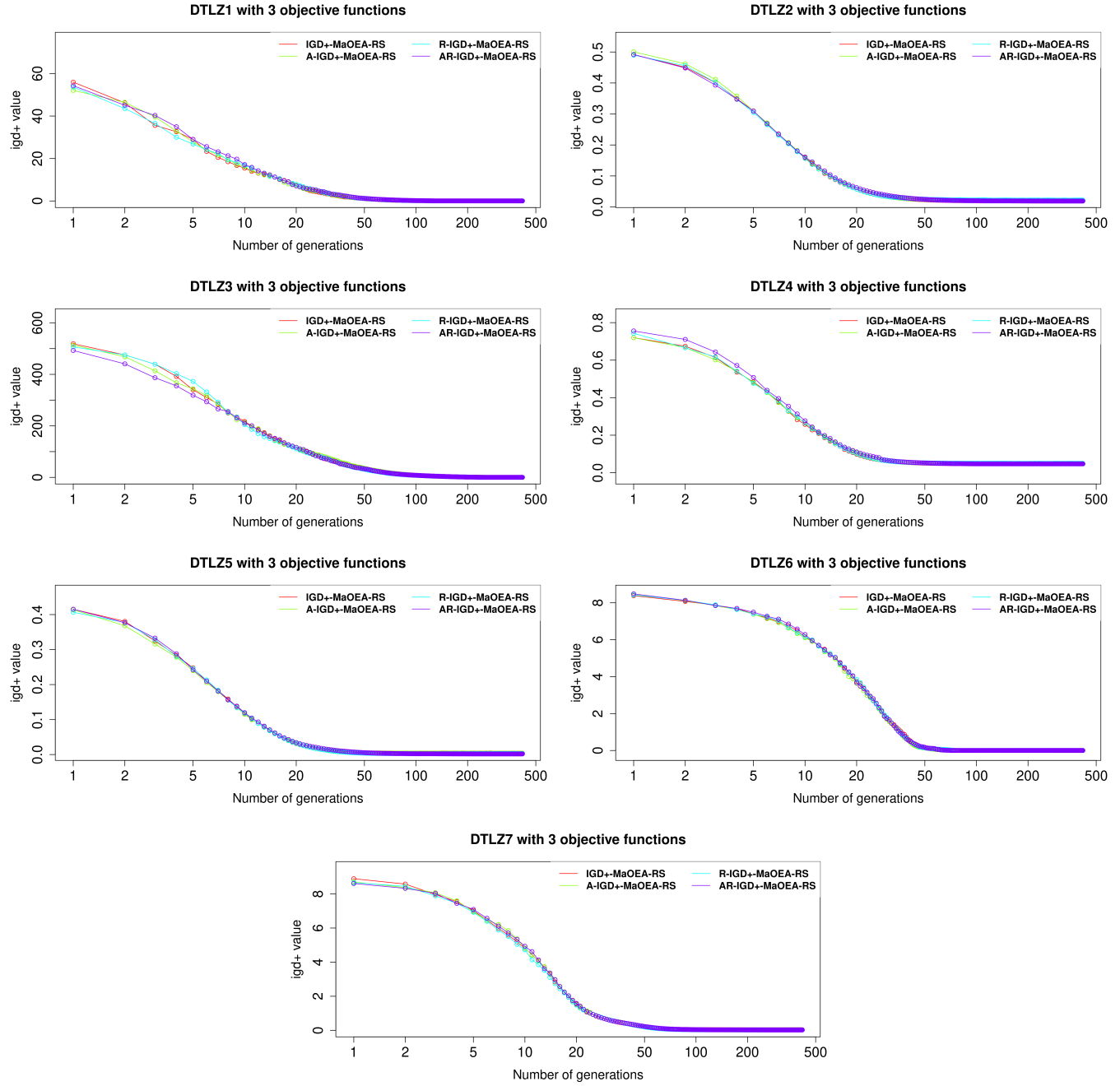


Fig. 5. Convergence graphs with the mean IGD^+ value of 30 independent runs on DTLZ1-DTLZ7.

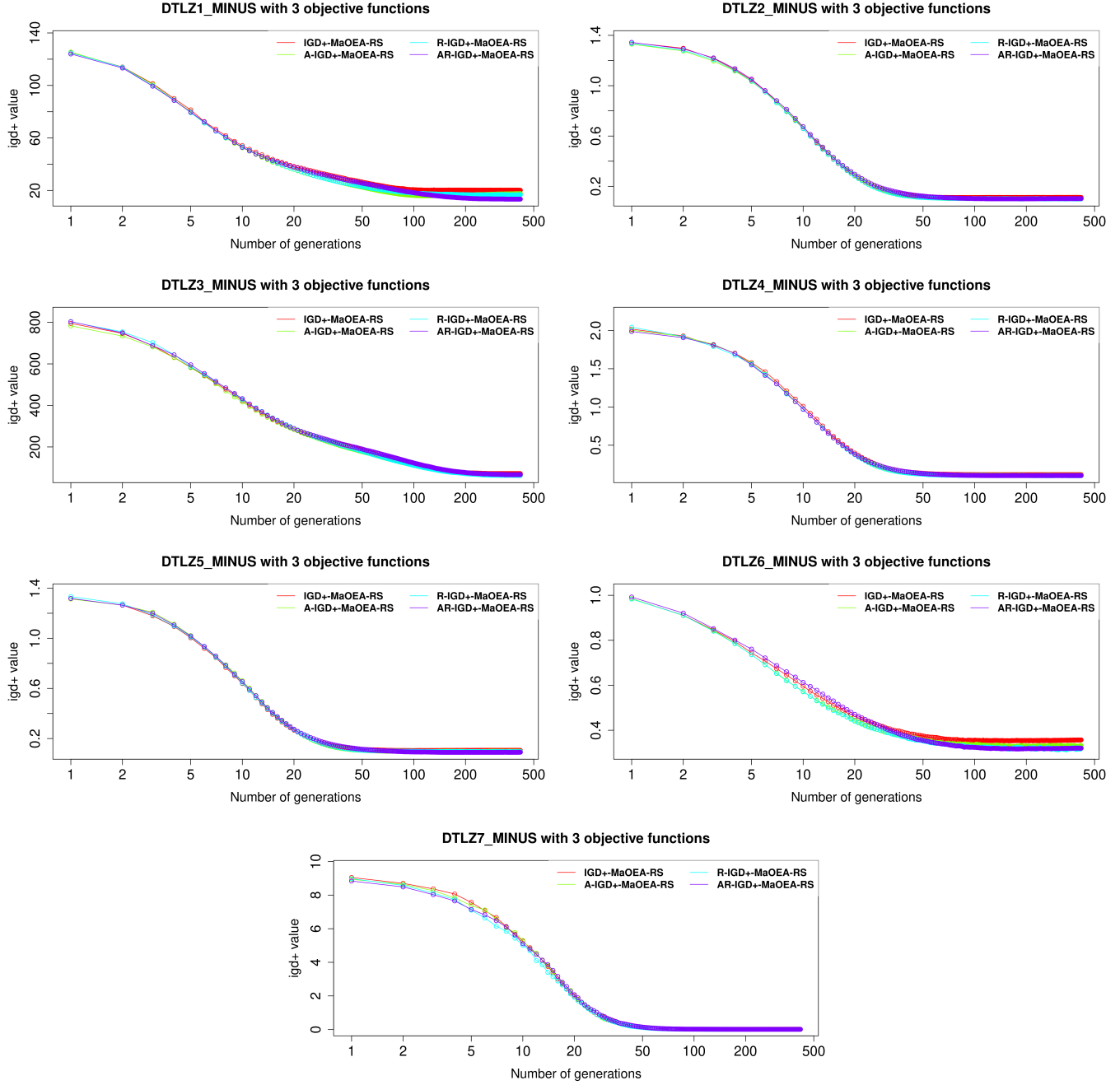


Fig. 6. Convergence graphs with the mean IGD^+ value of 30 independent runs on $DTLZ1^{-1}$ - $DTLZ7^{-1}$.

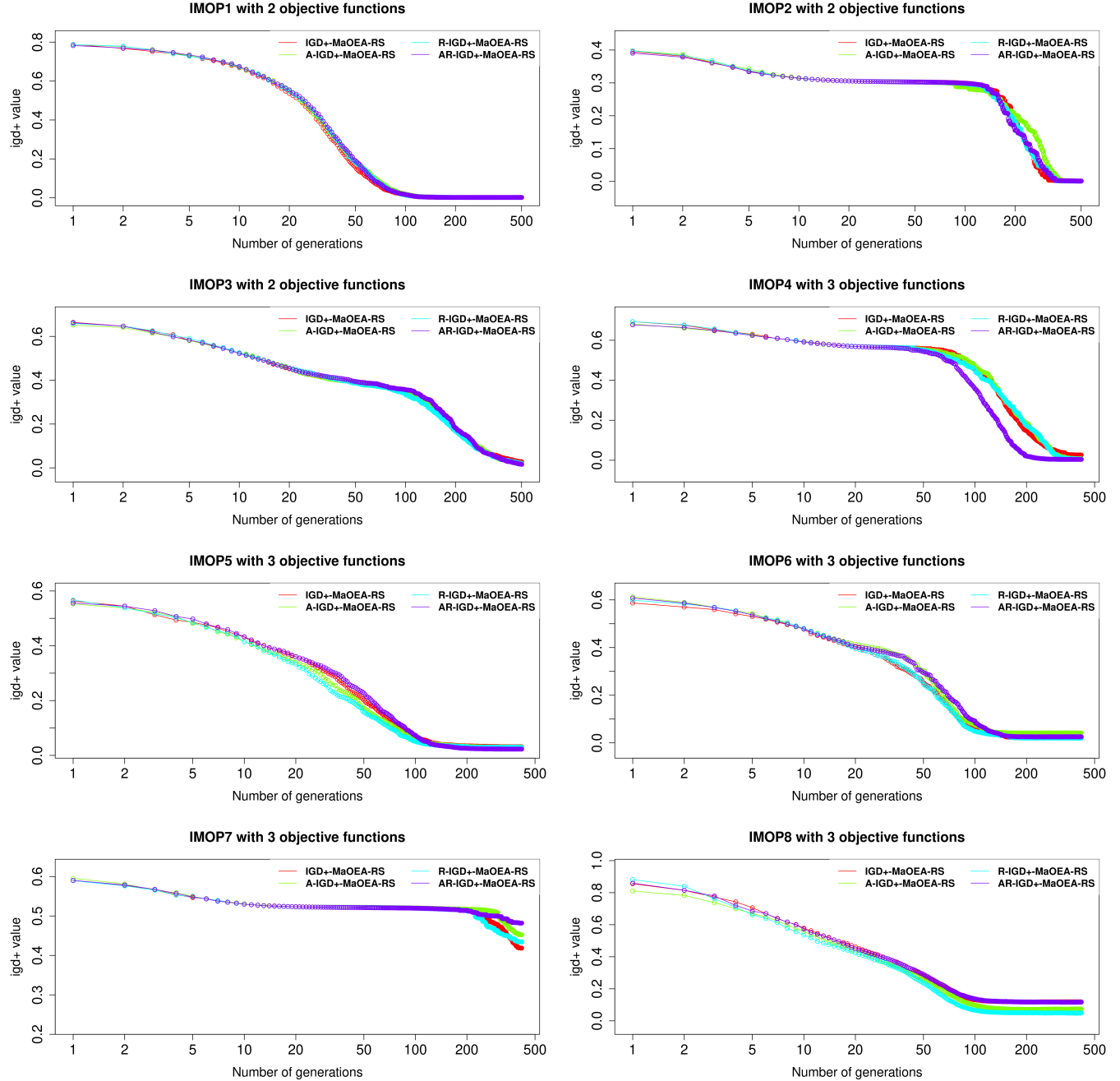


Fig. 7. Convergence graphs with the mean IGD⁺ value of 30 independent runs on IMOP1-IMOP8.